The use of proton microbeams for the production of microcomponents

T. Osipowicz [*], J.A. van Kan, T.C. Sum, J.L. Sanchez, F. Watt

Department of Physics, Research Centre for Nuclear Microscopy, National University of Singapore, Lower Kent Ridge, Singapore 119260, Singapore

Abstract

The recently developed process of high-energy ion beam micromachining (proton micromachining) is discussed. Proton micromachining is a novel process for the production of high aspect-ratio 3D microstructures. The sub-micron lateral resolution and the well-defined range of an MeV proton microbeam are utilized to make lithographic structures in suitable polymers (e.g., SU-8, PMMA). Sub-micron structures with a depth of tens of microns and aspect-ratios approaching 100 have been achieved. The use of different energies for multiple exposures allows the production of intricate 3D multi-layer structures in a single polymer layer, and because no mask is needed the process offers a wide range of possible geometries for the production of non-prismatic or even rounded features. The throughput of the technique does not compare favourably with conventional (masked) processes for high volume batch production of microcomponents. On the other hand, significant applications of high-energy ion beam micromachining may be developed, e.g. for the rapid production of prototypes, the research into the characteristics of microstructures, and the manufacture of molds, stamps and X-ray masks. © 2000 Elsevier Science B.V. All rights reserved.

PACS: 07.10.Cm; 07.78.+s; 85.40.Hp
Keywords: Micromachining; Nuclear microscope; High aspect-ratio

1. Introduction

Many innovative efforts are currently under way to develop technologies for the production and integration of microstructures and microelectromechanical systems (MEMS). It is expected that miniaturised sensors of various types (e.g. chemical, optical, acoustical or mechanical) and actuators will be integrated with microelectronic devices and that from such innovative MEMS applications new high-technology growth areas of enormous potential will develop, perhaps comparable to the development of microelectronics over the last three decades.

So far, commercially successful MEMS applications have almost exclusively used the so-called silicon-based MEMS technologies to produce devices, e.g. pressure sensors or accelerometers. The availability of the highly developed optical lithography technology allowed the production of such "shallow" structures without the need for

---

[*] Corresponding author. Tel.: +65-874-6745; fax: +65-777-6126.
E-mail address: phyto@leonis.nus.edu.sg (T. Osipowicz).

novel lithographic processes. However, the lateral resolution of optical lithography is limited by diffraction effects, structure sizes below about 100 nm are essentially out of reach.

High aspect-ratio 3D microstructures can presently be produced by a few technologies only, the best known of which is LIGA (the German acronym LIGA stands for Lithography, Electrodeposition and Molding) [1,2]. LIGA is a combination of deep X-ray lithography with electroplating and micromoulding that has emerged as an important technique for the fabrication of microstructures with large structural heights (typically 300–500 μm), lateral dimensions ranging from a few microns to hundreds of microns, and aspect-ratios up to 100. One of the limitations of the LIGA process is the restricted geometry of the microstructures that can be fabricated (essentially prismatic), this is a consequence of the masked deep X-ray lithography technique which is the first step in LIGA. Because of the relatively high costs associated with LIGA (a synchrotron X-ray source and sophisticated mask production facilities are required), simpler and more cost-effective 3D microstructure fabrication techniques are highly desirable.

Deep UV lithography is a process that employs higher energy photons than photolithography and therefore has a larger accessible depth and produces comparatively less diffraction effects, while avoiding the need for the typically very expensive X-ray source (synchrotron) needed for LIGA. Special resists are used which are partially transparent to UV, thereby allowing the UV radiation to penetrate deep into the resist for 3D exposures. The success of the technique, however, depends on the development of a suitable resist which is not only sufficiently transparent to UV light but also sensitive enough so that high-resolution structures can be made. The sensitivity of a resist can be improved many-fold using chemical amplification, a process where a single photon initiates a cascade of chemical reactions to increase scissioning (for positive resists), or cross-linking (for negative resists). Negative resists such as SU-8 are proving very successful for deep UV lithography; aspect-ratios of 10 can be currently achieved using deep UV lithography. This paper discusses the recently developed technique of proton micromachining [3] that utilises a focused light ion beam in the MeV energy range to produce 3D microstructures in a lithographic process. The use of a Nuclear Microscope for maskless lithography was initialised by Breese et al. [4,5] and further demonstrated by Mason et al. [6]. Since 1995 the field has been a major focus of the Research Centre for Nuclear Microscopy in Singapore [3,7–12]. Here, recent results of proton micromachining in Singapore are described, and recent improvements and plans for further developments of the facility are outlined. Furthermore, several micromachined test structures are shown that demonstrate the utility of the process in diverse application areas. Finally we assess areas where proton micromachining shows potential for commercial exploitation.

2. Irradiation procedures

The lithographic irradiations were carried out at the Research Centre for Nuclear Microscopy [13] in Singapore. Utilising a single ended Van de Graaff accelerator (HVEE AN 2500) and a high excitation coupled triplet quadrupole lens system (OM150), spot sizes close to 100 nm for 2.0 MeV protons were previously achieved at 100 pA beam current [14]. Preliminary work in proton micromachining was done using the magnetic scanning coils driven by the PC-based OMDAQ hard- and software package that was developed for analytical applications of the microprobe. This system limits the scan resolution to 256×256 pixels, and it readily became apparent that higher resolutions are needed for lithographic applications. A new scanning system was developed, based upon a Keithley ADD-16 DAC card, with a resolution of 12 bits per channel and a minimum dwell time of 300 μs. This system can generate scan resolutions up to 4096×4096, and it also allows the implementation of optimised scanning algorithms that minimise the occurrence of artifacts in the developed microstructures. A more detailed description of the scanning system can be found elsewhere [7]. The currents typically used for micromachining range from 1 to 100 pA with a beam-spot size about 1 μm^2. The structures shown

in this paper were made using the newly developed, negative-type resist SU-8 that requires a dose of 10 nC/mm^2 [11], a much lower proton dose than needed for the more conventional PMMA ($\sim$100 nC/mm^2) [11]. Areas of 400 $\times$ 400 μm^2 were exposed using a resolution of 512 $\times$ 512 pixels.

A belt-driven Van de Graaff accelerator generates the ion beam used for the exposures. This type of accelerator generally exhibits undesirable energy fluctuations and consequently produces beams with intensity fluctuations which are typically in the tens of Hz frequency range. In order to achieve accurate exposure doses, we employ two types of beam normalisation procedures: (a) normalisation of the dose/pixel using backscattered protons for direct normalisation or (b) measurement of the total beam charge in a rapid and typically more than 100 times repeating scanning procedure [7]. The latter method was used in all exposures shown in this paper. In order to exploit the geometrical freedom that a maskless process allows, the samples were mounted on a eucentric goniometer that has a 14 mm translational range for both the x and the y direction and allows rotations up to 40° around both the x and the y axis with a resolution of 0.1 mrad.

3. Multilayer structures

Several test structures were produced to demonstrate the versatility and adaptability of proton micromachining.

Fig. 1 shows an SEM micrograph of a set of suspended bars of different lengths produced in a single 36 μm thick SU-8 layer applied on a Si wafer. Such multi-layered structures are produced using multiple exposures at different proton energies. Two exposures were carried out in this case with 1.0 and 2.0 MeV protons. The 1.0 MeV protons have a range of about 22 μm in the SU-8 layer and therefore 1.0 MeV protons were used to produce the suspended bars. The supporting structure was exposed using 2.0 MeV protons, which penetrated through the SU-8 layer into the substrate. The cantilevers have a length between 51 and 242 μm, a width of 10 μm and a height of 22 μm. The microbeam system has to be refocused

after the energy change that follows the first exposure. This is currently done on a 2000 mesh Au grid that is moved into the beam spot, after removal the sample. When the new focus is established, the sample is moved back in the beam-spot, and that implies that the alignment between multiple exposures is critical. It was achieved by means of a marker on the resist layer, which is mapped using particle induced X-ray emission (PIXE) or backscattered protons (RBS). Suspended bars and cantilever structures made in this way were used to measure mechanical properties (e.g. Young's modulus) of SU-8 microstructures as a function of the ion dose [10].

Fig. 2(a) shows a buried microchannel structure that was produced in a similar fashion, using a 2 MeV proton beam to produce the supporting structure and 0.6 MeV protons to cross-link the rectangle that covers the channel. The inset (Fig. 2(d)) shows an optical micrograph of the structure. Because the SU-8 resist is semitransparent, the whole microchannel is visible in this image. The insets Fig. 2(b) and (c) shows more detailed SEM images of the exit and the entrance openings of the microchannel. It is expected that such structures will have applications in microfludic systems, e.g. in chip-cooling devices or in chemical microsensor systems.

Fig. 3 shows an example of an intricate multilevel anchored grid structure made by proton micromachining. Three different proton energies were used in one single layer of resist to produce this structure. In Fig. 3(a) an overview of the complete structure is shown. At the centre of the structure, two anchors produced using 2.0 MeV protons can be observed. Fig. 3(b) shows in more detail the region dotted white in Fig. 3(a), while Fig. 3(c) shows a schematic overview of the supported multilevel grid. Fig. 3(d) shows the structure seen along the direction of the black arrow in Fig. 3(a). Protons with an energy of 600 keV have a range of less than 10 μm in SU-8; this energy was used to produce the shallowest structures. The walls perpendicular to the first set were exposed with a 1.0 MeV proton beam resulting in 22 μm walls. The individual lines have a width of 5 μm and a spacing of 20 μm. The grid is suspended by the two anchors, 50 $\times$ 200 μm^2 each,
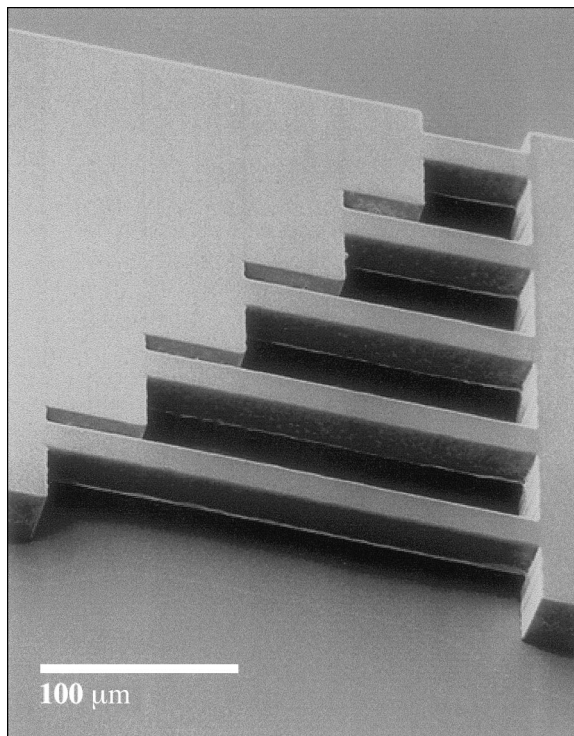
Fig. 1. SEM image of suspended beams in SU-8, produced by two ion beam exposures at 1 and 2 MeV proton energies.

and a typical exposure time for this whole structure is 40 s using a current of 100 pA. The scan pattern used to expose the 22 μm walls is sketched in Fig. 3(e), and the side of the structure on which the beam "jumped" to the next beam is seen in Fig. 3(d). Artifacts of the scanning process are clearly visible in Fig. 3(d): because the ion beam is continuously irradiating the structure, there is a residual dose delivered to the regions where the beam "jumps" from one beam to the next, and also, to some degree, because of the inductive time constant of the magnetic scanning system. In Fig. 3(d), a broadening of the lower part of the beam is clearly visible, and even a suspended structure is seen in the leftmost gap. In order to avoid such artifacts of the scanning process, a beam blanking system is currently being implemented that will allow to steer the beam off the sample when such "jumps" occur. At the same time, improvements to the scanning algorithm will be implemented so that the irradiation process is interrupted for a suitable amount of time after a "jump" so that the current in the scanning coils reaches its steady-state value.

Fig. 4 shows double-layered structures produced in a 36-μm layer of SU-8. The top layers, consisting of interconnected elongated ring-structures, were exposed with a 600 keV proton beam. These rings have a height of almost 10 μm and a width of 15 μm. They are supported by straight walls which were produced using a 2.0 MeV proton beam. The supporting walls have a length of 380 μm and a width of 10 μm. The upper exposure in Fig. 4 was carried out with the 2.0 MeV proton beam perpendicular to the resist, while for the lower structure shown in Fig. 4 the sample normal was tilted at an angle of 40° with respect to the 2 MeV proton beam. Such tilted structures can obviously not easily be produced by a mask-projection technique because of the edge effects that the mask will produce when irradiated at non-normal angle of incidence.
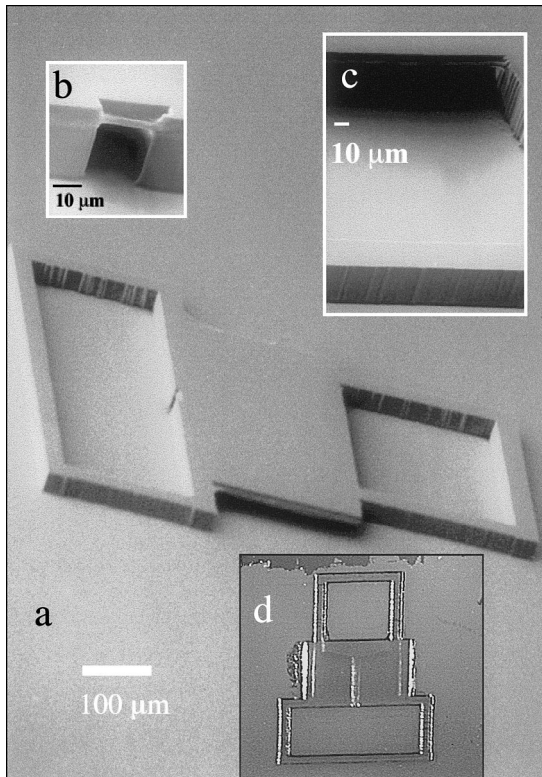
Fig. 2. Microchannel structure: (a) SEM overview, (b) channel exit (left in a), (c) channel entrance (right in a), and (d) optical micrograph seen from above the structure, the channel is visible in its entirety.

4. Potential applications of proton micromachining

The main consideration that one has to keep in mind when trying to identify commercial applications for proton micromachining is that, due to its "direct write" feature, the technique is far slower than masked projection techniques, and that in industrial mass production processes high throughput capabilities are essential. In spite of this, there are several applications for which proton micromachining seems well adjusted. These include:

LIGA mask production: The production of the masks needed for LIGA is a highly complicated process: a typical X-ray mask needs to be extremely stable under a high radiation load, have sub-250 nm pattern dimensions, and absorbing structures thick enough to attenuate the X-rays in certain regions. This implies that tens of micrometers thick layers of e.g. Au have to be structured. Proton micromachining has the potential to manufacture such masks. All these points can be made, to a somewhat lesser extent, as lower X-ray energies are used, for X-ray lithography as well.

Fundamental research: The rapid development of MEMS technologies generates, but also needs, an improved knowledge of the properties of microstructures: mechanical properties of beams and cantilevers, characteristics of fluid flows in microchannels, optical properties, wear characteristics of moving parts, inertial properties, etc. Basic research in these fields does not need high volume production, but relatively uncomplicated production of custom-built structures may prove highly advantageous.

Prototype production: The rapid and efficient development of working prototypes is critical for the rapid expansion in the batch production of microcomponents. The latter invariably involves high capital equipment expenditure. For prototypes, there is no need for batch manufacture, since the emphasis is then on product development rather than mass production, and it is in this area that direct-write processes may have both cost and time advantages.

Stamp and mold manufacture: Proton micromachining has the potential to manufacture individual 3D stamps or molds, which can then be used repeatedly for batch and high volume production. Current projects at the Research Centre for Nuclear Microscopy include development of 3D substrates for tissue engineering, precision molds for IC packaging, and microchannels for advanced electrophoresis applications.

5. Conclusions and outlook

In conclusion, recent test structures produced by proton micromachining are discussed. The unique characteristics of the technique, which combines sub-micrometer lateral resolution, high aspect-ratio capability and the geometrical freedom typical for direct-write processes are
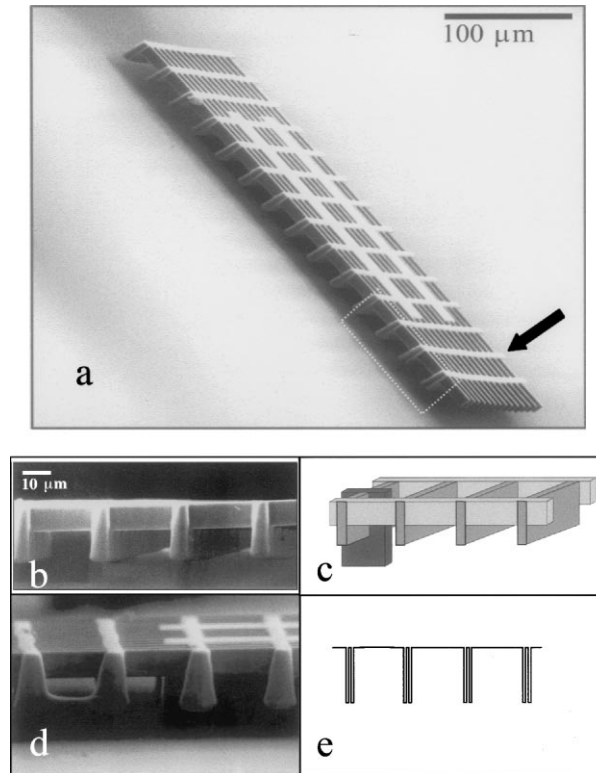
Fig. 3. SEM images of a level microgrid, produced by three exposures at 0.6, 1.2 and 2 MeV proton energy: (a) overview of the structure, (b) detail of the microgrid in (a), (c) design sketch of (b), (d) detail as seen along the arrow in (a), and (e) the scan path used to expose the 22 μm bars.
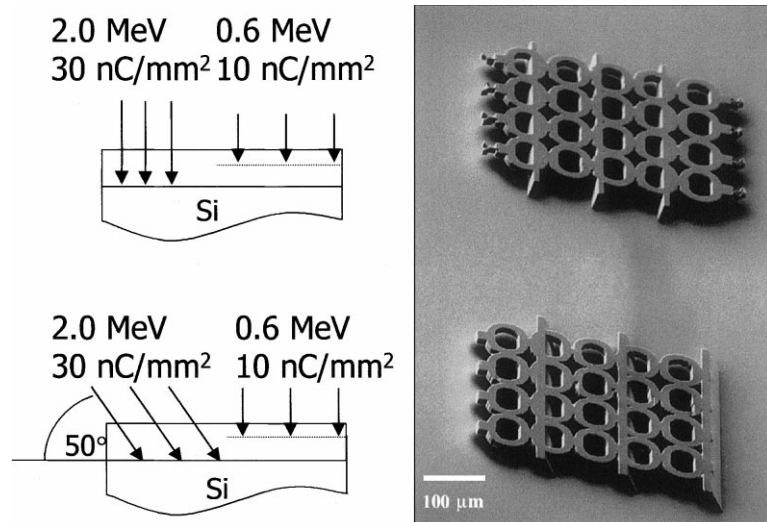

Fig. 4. Tilted and straight walls supporting an interconnected extended ring structure. The vertical walls in the upper exposure were done with the proton beam along the sample normal, and at an angle of 40° in the lower exposure.

demonstrated. The well-defined range of the proton beam allows the generation of complex multi-layered structures in a single resist layer. This enables the construction of slots, channels, holes, etc. with a well-defined depth. Although the procedure is generally slower than masked processes for bulk production, it is very suitable for rapid prototyping and the manufacture of molds, stamps and possibly LIGA masks.

Currently a highly stable 3.5 MV accelerator [15] is being installed at the Research Centre for Nuclear Microscopy. This machine will increase the capabilities of proton micromachining at the facility: Structures of increased depth of up to 160 µm will be produced with 3.5 MeV protons, coupled with improved definition in walls and edges consistent with the enhanced beam intensity stability.

References

[1] E.W. Becker, W. Ehrfeld, P. Hagmann, A. Maner, D. Münchmeier, Microelect. Eng. 4 (1986) 35.

[2] W. Ehrfeld, H. Lehr, Radiat. Phys. Chem. 45 (1995) 349.

[3] S.V. Springham, T. Osipowicz, J.L. Sanchez, L.H. Gan, F. Watt, Nucl. Instr. and Meth. B 130 (1977) 155.

[4] M.B.H. Breese, G.W. Grime, F. Watt, D. Williams, Nucl. Instr. and Meth. B 77 (1993) 169.

[5] D.G. de Kerckhove, M.B.H. Breese, M.A. Marsh, G.W. Grime, Nucl. Instr. and Meth. B 136 (1998) 379.

[6] L.M. Mason, A. Roberts, D.N. Jamieson, A. Saint, in: J.S. Williams, R.G. Elliman, M.C. Ridgway (Eds.), Ion Beam Modification of Materials, ISBN: 0-444-82334-4, North-Holland, 1996, p. 1110.

[7] J.L. Sanchez, J.A. van Kan, T. Osipowicz, S.V. Springham, F. Watt, Nucl. Instr. and Meth. B 136–138 (1998) 385.

[8] J.A. van Kan, J.L. Sanchez, B. Xu, T. Osipowicz, F. Watt, Nucl. Instr. and Meth. B 148 (1999) 1085.

[9] J.L. Sanchez, G. Guy, J.A. van Kan, T. Osipowicz, F. Watt, Nucl. Instr. and Meth. B 158 (1999) 185.

[10] J.Z. Yang, E.H. Tay, J.A. van Kan, J.L. Sanchez, F. Watt, to be published.

[11] J.A. van Kan, J.L. Sanchez, B. Xu, T. Osipowicz, F. Watt, Nucl. Instr. and Meth. B 158 (1999) 179.

[12] F. Watt, Nucl. Instr. and Meth. B 158 (1999) 165.

[13] F. Watt, I. Orlic, K.K. Loh, C.H. Sow, P. Thong, S.C. Liew, T. Osipowicz, T.F. Choo, S.M. Tang, Nucl. Instr. and Meth. B 85 (1994) 708.

[14] F. Watt, T. Osipowicz, T.F. Choo, I. Orlic, S.M. Tang, Nucl. Instr. and Meth. B 136–138 (1998) 313.

[15] D.J.W. Mous, R.G. Haitsma, T. Butz, R.H. Flagmeyer, D. Lehman, J. Vogt, Nucl. Instr. and Meth. B 130 (1997) 31.